https://dx.doi.org/10.4314/dujopas.v10i1c.30
ISSN (Print): 2476-8316
ISSN (Online): 2635-3490
Dutse Journal of Pure and Applied Sciences (DUJOPAS), *Vol. 10 No. 1c March 2024*

Energy Convergence in a Structure Optimization and Vibrational Modes of Some Acene Molecules

Kassim L. Ibrahim[1*], G. Babaji[2], G.S.M. Galadanci[2], Raymond C. Abenga[3] and H. U. Jamo[1]

[1]Lecturer, Physics Department,
Kano University of Science and Technology,
Wudil, Kano,
Nigeria.
Orcid ID: 0009-0005-8803-5500

[2]Department of Physics,
Bayero University Kano,
Nigeria.

[3]Department of Pure and Applied Physics,
Veritas University,
Abuja,
Nigeria.

Email: ikassim27@gmail.com

Abstract
Acene molecules, exhibit interesting electronic and structural properties due to the presence of alternating single and double bonds. There has been a recent surge in interest in studying small acenes, such as anthracene, tetracene, and pentacene. Geometry optimization and energy convergence for acene molecules are essential steps in understanding their properties and behavior. The modellings of MJs was done using Jmol computer code and the geometry of these structures was relaxed towards its minimum energy using a two-step procedures which are; pre-relax the structure with light settings and post-relaxation run using tight settings down to 10^{-2} eV/Å stopping criteria. The results showed that total energy uncorrected and the maximum force converged. The converged energies for anthracene, tetracene and pentacene molecules are, 0.0057 eV/Å, 0.0056 eV/Å, and 0.0060 eV/Å respectively. For the vibrational analysis, some of the results indicated that the input geometry is indeed a local minimum and not a saddle point. The results also showed a low IR absorption, with maximum intensity of 1.83 $D^2Å^{-2}$, 2.00 $D^2Å^{-2}$, and 1.91 $D^2Å^{-2}$ for anthracene, tetracene, and pentacene respectively.

Keywords: convergence, DFT, modelling, relaxation, vibration

INTRODUCTION
Geometry optimization plays a crucial role in computational physics or chemistry studies that involve electronic structure methods. It often contributes significantly to the computational cost of these studies, making efficient optimization algorithms highly desirable (Farkas and Schlegel, 2001). A basis set is a finite collection of atomic-like functions used to form the molecular orbital through a linear combination of atomic orbitals (LCAO). There are various options for basis sets, including Slater-type orbitals (STOs) and Gaussian-type Orbitals (GTOs). Wave functions, also referred to as stationary states or energy eigenstates, are essential in molecular modeling (Engel, 2002). They can be described by the time-independent

**Author for Correspondence*

Schrödinger equation (1), which is a fundamental equation in quantum mechanics that governs the behavior of electrons in molecules (Joita *et al.,* 2021). Understanding and solving this equation is crucial for determining the most accurate molecular structures and energetics (Kohn and Sham, 1965).

$$H\psi = E\psi, \quad (1)$$

where ψ is the state vector of the quantum system, E is the energy, and H is the Hamiltonian operator.

In the time-independent Schrödinger equation (Schrödinger, 1926), the operation may produce specific values for the energy called energy eigenvalues. In addition to its role in determining system energies, the Hamiltonian operator generates the time evolution of the wavefunction in the form:

$$H\psi = j\hbar\frac{\partial}{\partial t}, \quad (2)$$

where the j constant is the imaginary unit, $\hbar$ is the reduced Planck constant, and t is time.

The Schrödinger equation provides a method for calculating the wave function of a system and its dynamic change over time. The equation is a wave equation in terms of the wave function which predicts analytically and precisely the probability of events or outcome. The spatial part needs to be solved for in time-independent problems, because the time-dependent phase factor is always the same.

Acenes are polycyclic aromatic hydrocarbons that has been utilized in various nano applications due to their electronic properties. These families have shown high charge carrier mobilities, making them suitable for high-performance organic electronic devices. Acenes are a subclass of organic semiconductors formed out of several adjacent benzene rings organized in a row. Acene molecules, exhibit interesting electronic and structural properties due to the presence of alternating single and double bonds. Understanding the stability and energy states of these molecules is crucial for predicting their behavior in different environments and applications. In this context, geometry optimization (Abegg, and Ha, 1974), energy convergence (Jäntschi, 2011), and vibrational analysis (Russ *et al.,* 2004), are essential tools to investigate the structural and energetic aspects of acene molecules. Due to the instability of large acenes, these attempts have, unfortunately, not been very successful. Therefore, there has been a recent surge in interest in studying small acenes, such as anthracene (Ibrahim *et al.,* 2022), tetracene (Yelin *et al.,* 2021), and pentacene (Pinheiro *et al.,* 2020).

Geometry optimization and energy convergence for acene molecules are essential steps in understanding their properties and behavior (Lassnig, *et al.,* 2015). These processes help scientists predict the most stable structures and energy states of these molecules, which can be applied in various fields, such as material science, pharmaceuticals, and organic chemistry.

METHODS

This work involves a modelling of molecule and extended structure of molecular junction, Density Functional Theorem (DFT) calculations. The procedures followed in conducting this research are structure modelling, structure relaxation calculations, and vibrational analysis.
The modellings of MJs was done using a computer code Jmol.14.6.4 version. The geometry of these structures was relaxed towards its minimum energy. In this relaxation runs, a two-step procedure was followed as;

- Pre-relax the structure with *light* settings down to 10^{-2} eV/Å.
- This is then followed by post-relaxation run using *tight* settings.

For relaxing the geometry, a keyword "relax_geometry", specifies a geometry relaxation using bfgs algorithm, together with a standard convergence criterion for the forces in the final

geometry. Thus, no force component for any atom of the relaxed structure should exceed 10^{-2} eV/Å. The extended structures of molecular junctions are formed using Au-clusters as source and drain electrodes (Stegmann *et al.,* 2020). DFT electronic structure calculations were performed as implemented in the FHI-aims computer program (Blum *et al;* 2009), with the Perdew-Burke-Ernzerhof (PBE) exchange correlation functional to ensure accuracy and reliability.

1. Geometry optimization: This involves finding the most stable arrangement of atoms in the acene molecule. To do this, FHI-aims.081912.serial.x were used throughout. These programs employ algorithms to minimize the energy of the molecule by adjusting the positions of the atoms. The optimization process continues until the forces acting on each atom are minimal or close to zero.
2. Energy convergence: After the geometry optimization, it is crucial to ensure that the calculated energy values have converged within the force tolerance specified by *relax_geometry,* which in this case is $1x10^{-2}$. Convergence can also be achieved by refining the basis set, increasing the number of k-points (in the case of periodic systems), or improving the numerical accuracy of the calculations.

RESULTS AND DISCUSSION

The starting geometries was built and cleaned with a modelling and visualization software called Jmol. As such the geometry was generated with a certain degree of distortion, thus need to be optimized and relaxed to a minimum energy level. Both geometries were optimized and presented here.

Geometry Optimization and Relaxation

The geometry of the starting molecules were first optimized using tier 1. They were optimized again using tier 2.

Tables 1, 2, and 3 are the results summary for the geometry optimizations and relaxations steps of an anthracene, tetracene, and pentacene molecules respectively. These results include the first (pre-relaxation) and the second (post-relaxation) relaxation steps.

Table 1: Results from optimizing anthracene molecule.

S.No.	Quantity	Pre relaxation	Post relaxation
1	Number of Self_Consistency cycles	107	71
2	Number of relaxation steps	11	7
3	Total time (wall_clock)	545.946 s	3495.463s
4	Total number of basis functions	246	696
5	Species_default	First tier (*light)*	Second tier (*tight)*
6	Total energy	-14677.235744189 eV	-14678.134878444 eV

Table 2: Results from optimization of tetracene molecule.

S.No.	Quantity	Pre relaxation	Post relaxation
1	Number of Self_Consistency cycles	113	76
2	Number of relaxation steps	12	6
3	Total time (wall_clock)	961.128 s	4271.556 s
4	Total number of basis functions	312	882
5	Species_default	First tier (*light)*	Second tier (*tight)*
6	Total energy	-18856.807608322 eV	-18857.970191034 eV

Table 3: Results from optimization of pentacene molecule.

S.No.	Quantity	Pre relaxation	Post relaxation
1	Number of Self_Consistency cycles	118	119
2	Number of relaxation steps	11	12
3	Total time (wall_clock)	1728.653 s	8341.363 s
4	Total number of basis functions	378	1068
5	Species_default	First tier (*light*)	Second tier (*tight*)
6	Total energy	-23036.348708529 eV	-23037.780826424 eV

Even though, the number SC-cycles and the number of relaxation steps reduced in the post relaxation, the total or wall_clock time multiplies in reference to that of pre-relaxation for all molecules. Energy is converged to a minimum possible value during the post relaxation process. The number of Self_Consistency cycles and total time increases with increase in the number of benzene rings (i.e., size of the molecule) in a molecule while the number of relaxation steps is independent of molecular size. The total energy uncorrected for the optimized structures of anthracene, tetracene, and pentacene molecules are found to be -14678.134878444 eV, -18857.970191034 eV, and -23037.780826424 eV respectively. This claim is supported by Donatella *et al.,* (2021).

Energy and Force Convergence

The total energy uncorrected and the maximum force converged. Results for the convergence of these energies and forces are illustrated in Figure 2. Maximum force converged from 2.29 eV/Å to 0.0099 eV/Å for anthracene molecule, 2.24 eV/Å to 0.0084 eV/Å for tetracene molecule and 2.45 eV/Å to 0.0091 eV/Å for pentacene molecule during pre-relaxation process. In the post-relaxation process (Figure 3), these forces were further converged 0.0057 eV/Å, 0.0056 eV/Å, and 0.0060 eV/Å for anthracene, tetracene, and pentacene molecules respectively.

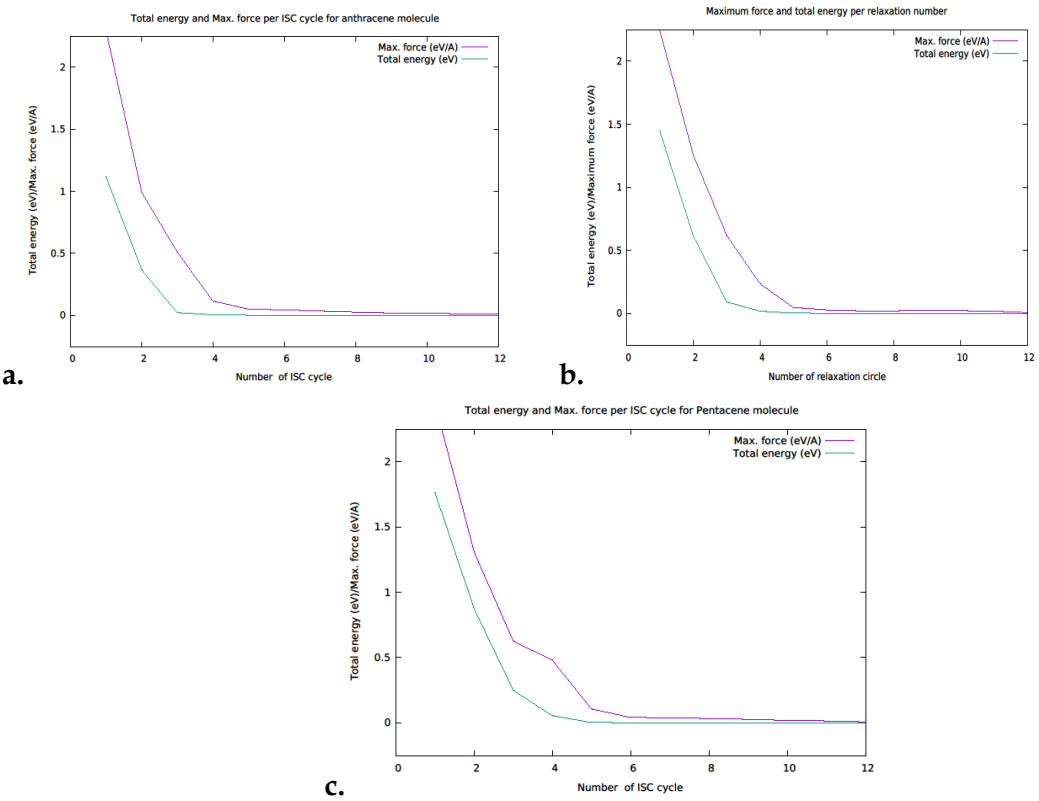

Figure 2: Energy and maximum force convergence for anthracene (a), tetracene (b), and pentacene molecules for pre-relaxation process.

As for energy during the pre-relaxation, it is converged from -14676.1167603398 eV to -14677.2357441892 eV for anthracene molecule, from -18855.3624815859 eV to -18856.8076083225 eV for tetracene molecule, and from -23034.5839891169 eV to -23036.3487085291 eV for pentacene molecule. Also it is converged again during the post-relaxation to -14678.1348784438 eV, -18857.9701910341 eV, and -23037.7808264236 eV for anthracene, tetracene and pentacene respectively. This is in total agreement with Case *et al.,* (2016) and Hirai *et al.,* (2022).

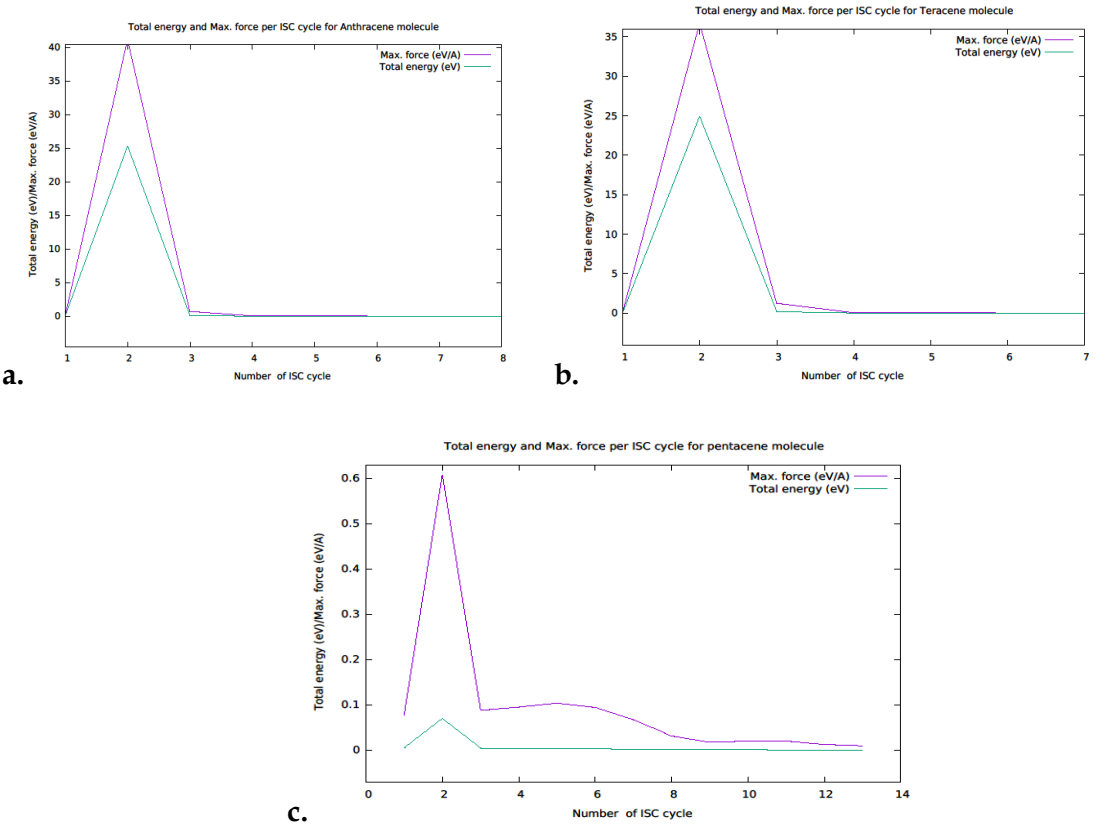

Figure 3: Energy and maximum force convergence for anthracene (a), tetracene (b), and pentacene molecules for post-relaxation process.

Figure 4, is the optimized structure for anthracene, tetracene, and pentacene. These are visualization result for the geometry which found in the geometry.in.next_next-step.

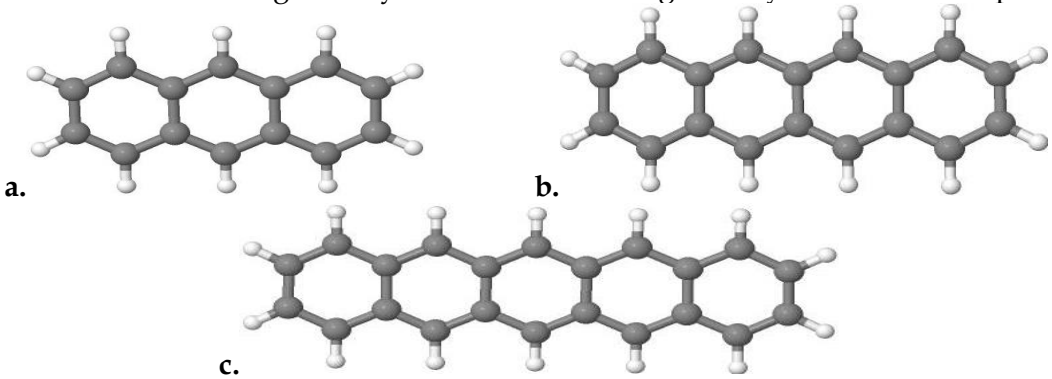

Figure 4: Optimized structures of anthrace (a), tetracene (b), and pentacene (c) molecules

Vibrational Analysis

The results for the vibrational analysis was presented in Figures 4, 5, and 6. In these Figures, the frequency for the vibration, zero-point energy, and IR-intensity absorption for each molecule are presented.

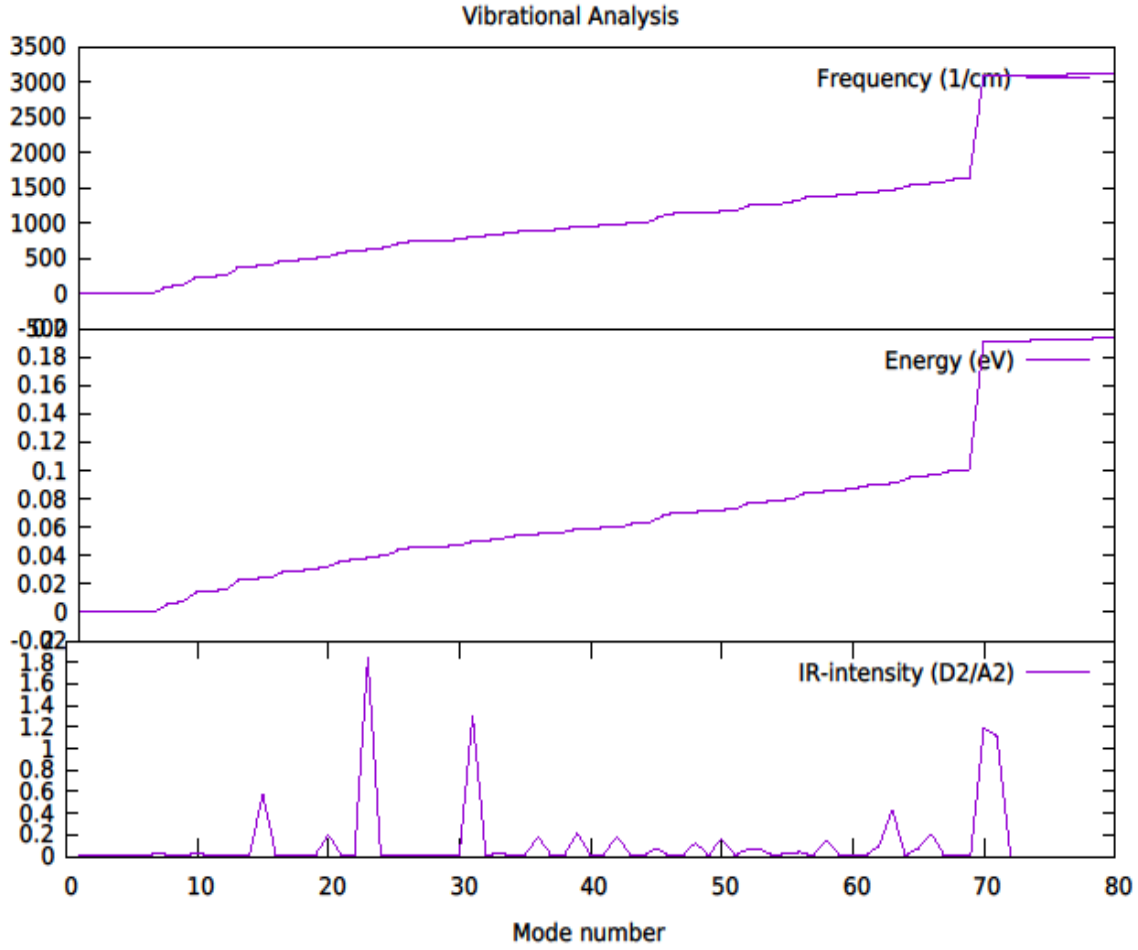

Figure 5: Frequency, zero-point energy and IR-intensity obtained in vibration of anthracene molecule

Figure 5 represent the frequency (cm^{-1}), the zero-point energy (eV), and the IR-intensity absorption for an anthracene molecule. A total of 72 vibrational modes were obtained. The first five frequency values are -2.93 cm^{-1}, -1.58 cm^{-1}, -0.87 cm^{-1}, -0.63 cm^{-1}, and -0.41 cm^{-1}. These negative values indicated that the input geometry is indeed a local minimum and not a saddle point. The maximum vibrational frequency value is found to be 3118.84 cm^{-1}, this is very close to the previously reported work by Gurku and Ndikilar, (2012). A significant raise in frequency from 1619.82 cm^{-1} to 3081.73 cm^{-1}, and energy from 0.10eV to 0.19eV occurs from mode number 62 to 63. This shows that the energy and frequency are in phase. As for the IR-intensity, the results shows a low IR absorption, with maximum intensity of 1.83 $D^2Å^{-2}$ at mode 23 which correspond to the frequency of 715.47 cm^{-1}.

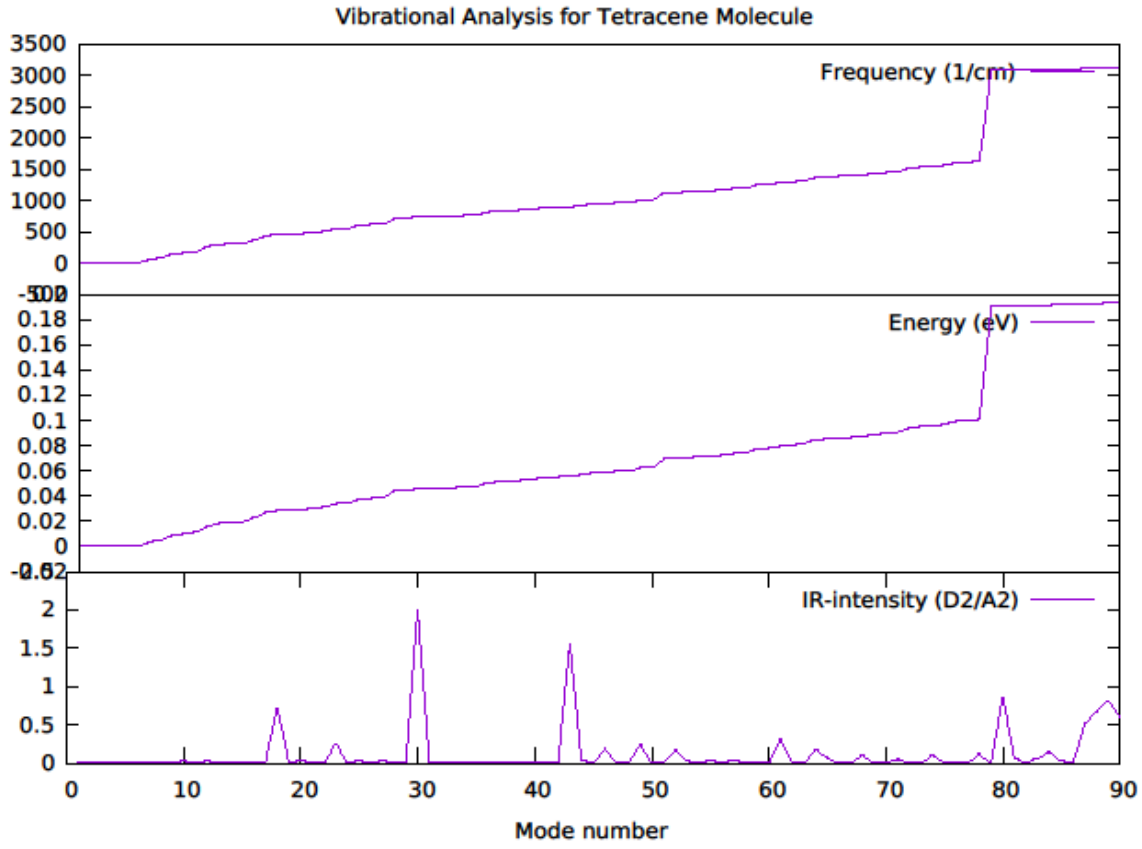

Figure 6: Frequency, zero-point energy and IR-intensity obtained in vibration of tetracene molecule

As for the tetracene molecule, the results for vibration is reported in Figure 6. Total of 90 vibrational modes were obtained, closer to that was obtained by Gidado *et al.,* (2017). The results showed that the first four modes has a negative frequencies of -1.52 cm^{-1}, -0.79 cm^{-1}, -0.64 cm^{-1}, and -0.33 cm^{-1} respectively and indicated that the input geometry is indeed a local minimum. The highest vibrational frequency is 3118.21 cm^{-1} and this is at mode number 90, which also corresponds to the 0.19 eV energy and IR-intensity of 0.58 $D^2Å^{-2}$. A significant shift in frequency from 1624.91 cm^{-1} to 3081.43 cm^{-1} and energy from 0.10 eV to 0.19 eV, occurred from modes number 78 to 79 respectively. These also means the frequencies are in phase with zero-point energies. For the vibrational analysis, the IR-intensity values showed that, tetracene molecule is a better IR absorber than the anthracene molecule, with the maximum IR-intensity of 2.00 $D^2Å^{-2}$ at 30th vibrational mode. This corresponds to the 734.00 cm^{-1} frequency and energy of 0.045 eV.

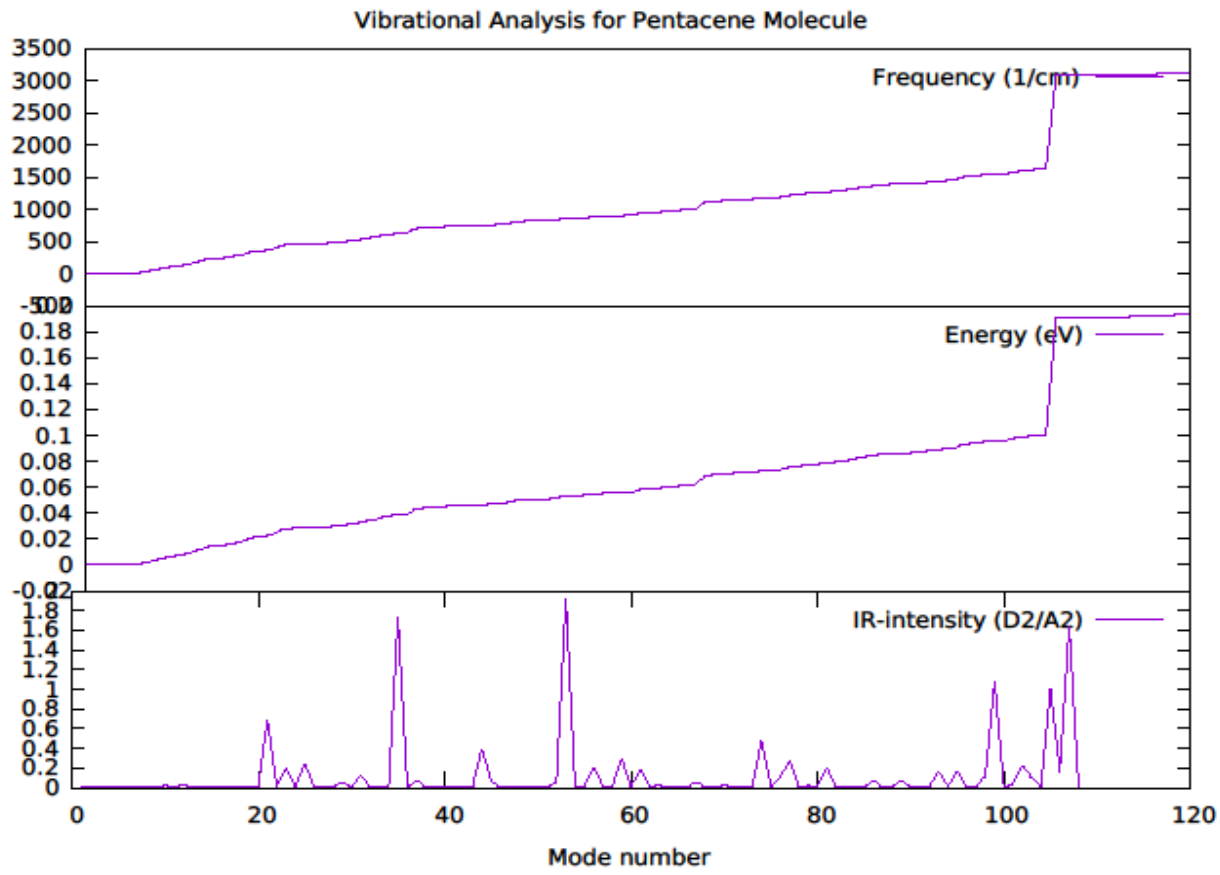

Figure 7: Frequency, zero-point energy and IR-intensity obtained in vibration of pentacene molecule

Pentacene on the other hand, has 108 vibrational modes, contrary to 102 obtained by Galadanci *et al.,* (2015). The vibrational analysis for the pentacene molecule is represented in Figure 7. It can be seen that the first three modes of frequencies are negative with values of -1.40 cm^{-1}, -0.78 cm^{-1}, and -0.43 cm^{-1} which correspond to the negative energies of -0.000087 eV, -0.000048 eV, and -0.000027 eV respectively. The negative values indicated that the input geometry is indeed a local minimum and not a saddle point. This result also showed that, the highest vibrational frequency is 3119.14 cm^{-1} at 108^{th} mode, and this corresponds to the energy of 0.19 eV and IR-intensity of 0.0089 $D^2Å^{-2}$. The frequency shift from 1619.67 cm^{-1} to 3082.22 cm^{-1} and that of the energy from 0.10 eV to 0.19 eV occurred vibrational modes of 94 and 95 respectively. The vibration results showed that there is a numerous reflexes for an IR absorption with the highest been 1.91 $D^2Å^{-2}$. This results are in partial agreement with the work by Babaji, (2015).

CONCLUSION

The results show that, apart from other convergence criteria, the time taken in geometry optimization and relaxation also depend on the molecular size. The number of Self Consistency cycles and total time increases with molecular size while the number of relaxation steps is independent of molecular size. The total energy uncorrected for the optimized structures of molecules is also dependent upon the molecular size.

For the vibrational analysis, the results showed that as the number of negative frequency values obtained reduces with the increase in molecular length, the values of the highest vibrational frequency is independent of the molecular length. It showed that vibrational frequency changes with the change of zero-point energy.

REFERENCES

Abegg, P.W. and Ha, T.-K. (1974). Ab initio calculation of spin-orbit-coupling constant from Gaussian lobe SCF molecular wavefunctions. Mol. Phys., 27, 763–767.

Babaji, G. (2015). SCF Cycle Convergence, Structure Optimization, and Vibrational Modes of Coumarin (*a*-Benzopyrone). *International Journal of Applied Physics and Mathematics,* 5(3), 206-217. DOI: 10.17706/ijapm.2015.5.3.206-217.

Blum, V., Gehrke, R., Hanke, F., Havu, P., Havu, V., Ren, X., and Reuter, M. S. (2009). Ab initio molecular simulations with numeric atom-centered orbitals. *Computer Physics Communications*, 2175-2196.

Case, D. H., Campbell, J. E., Bygrave, P. J., Day, G. M. (2016). Convergence Properties of Crystal Structure Prediction by Quasi-Random Sampling. *J Chem Theory Comput*. 9;12(2):910-24. doi: 10.1021/acs.jctc.5b01112.

Donatella Bálint and Lorentz Jäntschi (2021). Comparison of Molecular Geometry Optimization Methods Based on Molecular Descriptors. *Mathematics*, 9, 2855. https://doi.org/10.3390/math9222855.

Engel, E. (2002). Orbital-dependent functional for the exchange-correlation energy. In Fiolhais, C., Nogueira, F., & Marques, M. (Eds), *A Primer in Density Functional Theory*. Springer, Berlin.

Galadanci, G.S.M., Ndikilar, C. E., Sabiu, S.A., Safana, A. (2015). Molecular Dynamics and Vibrational Analysis of Pentacene: RHF and DFT Study. *Chemistry and Materials Research,* 7(11), 16–23.

Gidado, A. S., Abubakar, M., and Galadanci, G.S.M. (2017). Geometry Optimization and Vibrational Frequencies of Tetracene Molecule in Gas Phase and in Methanol Based on Density Functional Theory and Restricted Hartree-Fork. *Bayero Journal of Pure and Applied Sciences,* 10(1), 18–31.

Gurku, U., and Ndikilar, C. E. (2012). Electronic Structure and Properties of the Organic Semi-Conductor Material Anthracene in Gas Phase and Ethanol: An ab Initio and DFT Study. *The African Review of Physics,* 27 (7), 253–263.

Hirai, H., Horiba, T., Shirai S., Kanno, K., Omiya, K., Nakagawa, Y.O., Koh, S. (2022). Molecular Structure Optimization Based on Electrons-Nuclei Quantum Dynamics Computation. *ACS Omega*. 7(23), 19784-19793. doi: 10.1021/acsomega.2c01546. PMID: 35722014; PMCID: PMC9202041.

Ibrahim, K. L., Babaji G. and Nura A. M. (2022). Charge Transport Enhancement in Anthracene Molecular Junction: Density Functional Theory Studies. *J. Mater. Sci. Res. Rev.,* vol. 10, no. 4, pp. 32-41, 2022; Article no.JMSRR.95693.

Jäntschi, L. (2011). Computer assisted geometry optimization for in silico modeling. *Appl. Med. Inform*., 29, 11–18.

Joita, D.-M., Tomescu, M.A., Bàlint, D., and Jäntschi, L. (2021). An Application of the Eigenproblem for Biochemical Similarity. *Symmetry*, 13, 1849.

Kohn, W., and Sham, L. J. (1965). Self-consistent equations including exchange and correlation effects. *Phys. Rev., 140*, A1133.

Lassnig, R., Hollerer, M., Striedinger, B., Fian, A., Stadlober, B., Winkler, A. (2015). Optimizing Pentacene thin-film transistor performance: Temperature and surface condition induced layer growth modification. *Organic Electronics,* 26, 420–428.

Pinheiro, M., Machada, F.B.C., Plasser, F., Aquino, J.A., and Lischka, H. (2020). A system analysis of excitonic properties to seek optimal singlet fission: the BN-substitution patterns in tetracene. *Journal of Material Chemistry C*. DOI: 10.1039/C9TC06581D.

Russ, N.J., Crawford, T.D., and Tschumper, G.S. (2004). Real versus artifactual symmetry-breaking effects in Hartree–Fock, density-functional, and coupled-cluster methods. J. Chem. Phys., 120, 7298.

Schrödinger, E. (1926). An Undulatory Theory of the Mechanics of Atoms and Molecules. *Phys. Rev.*, 8, 1049–1070.

Stegmann, T., Franco-Villafane, J. A., Ortiz, Y. P., Deffner, M., Herrman, C., Kuhl, U., . . . Seligman, T. H. (2020). Current vortices in aromatic carbon molecules. *Physical Review B*, 075405-1-10.

Yelin T., Chakrabarti S, Vilan A., Tal O. (2021). Richness of molecular junction configurations revealed by tracking a full pull-push cycle. *Nanoscale*, 13, 18434-18440. DOI: https://doi.org/10.1039/D1NR05680H